NATIONAL ADVISORY COMMITTEE FOR AERONAUTICS

TECHNICAL NOTE 2001

AERODYNAMIC CHARACTERISTICS OF DAMPING SCREENS

By G. B. Schubauer, W. G. Spangenberg
and P. S. Klebanoff

National Bureau of Standards

Washington
January 1950

NATIONAL ADVISORY COMMITTEE FOR AERONAUTICS

TECHNICAL NOTE 2001

AERODYNAMIC CHARACTERISTICS OF DAMPING SCREENS[1]

By G. B. Schubauer, W. G. Spangenberg
and P. S. Klebanoff

SUMMARY

The experimental investigation of damping screens described herein was undertaken primarily to test theories of the effects of damping screens and to obtain information on the performance of screens in oblique flow. Data on normal- and tangential-force coefficients are given for a variety of square-mesh screens. Damping theories are reviewed and performance is compared with theory. The characteristics investigated include the damping of longitudinal and lateral components of turbulence, the effect of screens on scale, the conditions for the production of turbulence and eddies by screens, and the damping of spatial variations of mean speed.

INTRODUCTION

Within the last decade screens have found ever-increasing use in wind tunnels to reduce turbulence. As the result, the turbulence in many modern wind tunnels has been reduced to levels unknown 10 years ago. Along with the attainment of low turbulence came the recognition that low turbulence was a necessity for many wind-tunnel investigations. Much importance is therefore attached to the damping screen, and as much as possible should be known about its characteristics.

In earlier times, in fact dating from some of the earliest wind tunnels, screens were used to reduce differences in mean speed in order to obtain a more uniform stream. Prandtl (reference 1) appears to have been the first to obtain an expression for the reduction of these differences in terms of a coefficient, now commonly known as the pressure-drop coefficient. Collar (reference 2) obtained a different expression for the reduction of differences in mean speed involving this coefficient and showing fair agreement with his experimental results.

---

[1]Paper presented in part at the Seventh International Congress for Applied Mechanics, London, September 5-11, 1948.

A few years ago Taylor pointed out that there is not only a change in pressure but also a change in direction if a stream passes through a screen obliquely. Based on these two effects, a general theory of damping has recently been developed by Taylor and Batchelor (reference 3) which may be applied to the damping of turbulence as well as to the damping of mean spatial differences in velocity.

In 1940 a systematic investigation of the damping of turbulence was conducted at the National Bureau of Standards (reference 4). Screens consisting of various wire diameters and various numbers of wires per inch were placed in different numbers in the settling chamber of the tunnel shown in figure 1, and turbulence measurements were made in the test section. A simple theory, involving only the pressure-drop coefficient of a screen, was proposed on the assumption that a screen reduced the energy of turbulence irrespective of the distribution of the energy between longitudinal and lateral components. This theory was in good agreement with the experimental results.

The theory of Taylor and Batchelor deals with longitudinal and lateral components of the turbulence separately and predicts a significantly greater reduction in the longitudinal component than in the lateral component. The absence of such separate effects in the 1940 results does not necessarily disprove the theory. Taylor has pointed out that turbulence may become isotropic very quickly, and such differences, if they did exist, may not have been found because measurements were not made sufficiently near the screen. Most of the measurements were made in the test section of the tunnel about 18 feet from the nearest screen, and there was in addition a contraction of the stream with a possible effect on the relative magnitude of the components of the fluctuations.

It was decided, therefore, to conduct another experimental investigation on damping screens, this time avoiding a contraction and making measurements as near as possible to the downstream side of the screen. To obtain the information needed to apply the theory, it was necessary to measure the normal- and tangential-force coefficients for all of the screens used in the damping tests. Following Taylor's original observation that a stream meeting a screen at some angle to the normal was deflected toward the normal on passing through, an investigation of this effect was made by Simmons and Cowdrey (reference 5). It was felt that the effect was of sufficient importance to justify further study here.

The investigation was suggested by Dr. Hugh L. Dryden, following correspondence on this subject with Sir Geoffrey Taylor, and was conducted under the sponsorship and with the financial assistance of the National Advisory Committee for Aeronautics.

The authors wish to express their appreciation of the assistance and many helpful suggestions given by Dr. Dryden and Sir Geoffrey Taylor. Acknowledgment is extended to Miss Zulime W. Diehl and Messrs. I. A. Kenerson, M. J. Noble, and William Squire who assisted in carrying out the experimental program.

SYMBOLS

U	mean velocity averaged over time
$\bar{U}$	mean velocity averaged over time and space
u'	root-mean-square value of longitudinal turbulence fluctuations
v'	root-mean-square value of lateral turbulence fluctuations
f_u	reduction factor for u'
f_v	reduction factor for v'
f_{uv}	reduction factor with no distinction between damping of u' and v'
f_1	reduction factor for spatial variations in mean speed
f_2	reduction factor for spatial variations in mean direction
θ	angle of flow incidence measured from normal to screen
ϕ	angle of flow exit measured from normal to screen
δ	deflection at screen
α	limiting value of ϕ/θ as θ approaches zero
K_θ	pressure-drop coefficient when angle of incidence is θ and angle of exit is ϕ
K	pressure-drop coefficient when $\theta = 0$
F_θ	tangential-force coefficient when angle of incidence is θ and angle of exit is ϕ

Δp	pressure drop across screen
D	drag of wire forming one side of square mesh
d	screen wire diameter
N	number of wires per foot in screen
ρ	air density
ν	kinematic viscosity
R	Reynolds number (Ud/ν)
n	frequency
R_y	correlation coefficient for longitudinal fluctuations at two points separated by lateral distance y
L_y	integral scale of turbulence based on R_y

SCREEN COEFFICIENTS

Since flow through a screen can take place only in the spaces between wires, the resistance offered by a screen depends on its solidity, defined as the ratio of closed area to total area. The resistance is usually expressed in terms of the pressure drop occurring when a screen is in a duct with its plane perpendicular to the flow, and the expression commonly used is

$$\Delta p = \frac{1}{2}\rho U^2 K \qquad (1)$$

where K is a pressure-drop coefficient depending on the solidity of the screen and the Reynolds number.

Taylor has recently pointed out that a stream which approaches a screen at some angle to the normal will be deflected toward the normal on passing through. If θ is the angle of incidence, measured from the normal, and ϕ is the corresponding angle of exit from the screen, it is found that ϕ is less than θ. Since this deflecting phenomenon is now recognized as an important characteristic of a screen, it becomes

desirable to specify the associated tangential-force coefficient F_θ. This is given by the following equation, derived in reference 3 by considering the change in momentum across the screen:

$$F_\theta = 2\frac{\cos\theta}{\cos\phi}\sin(\theta - \phi) \qquad (2)$$

Under these conditions the pressure-drop coefficient will also depend on θ. It is again given by equation (1) where it will be denoted by K_θ when the velocity U makes the angle θ to the normal on the upstream side and the stream leaves the screen at the angle ϕ. For an arbitrary angle θ, there are then both the normal- and tangential-force coefficients, designated by K_θ and F_θ, where both are functions of θ as well as of the solidity and Reynolds number.

Both F_θ and K_θ were determined for the screens listed in table 1. The setup used is shown diagrammatically in figure 2(c). The measurements were made at the end of a 12-inch-square duct discharging into free air, the end of the duct being cut off successively at various angles, corresponding to θ, and the various screens being placed over the end of the duct. Precautions were taken to secure a uniform velocity distribution upstream from the screen with thin boundary layers. Sample traverses immediately upstream from the duct exit are shown in figure 2(a). Various airspeeds were used up to a maximum of 40 feet per second.

To determine K_θ, both static and dynamic pressures were measured upstream, and the static pressure was measured downstream from the screen at the midpoint. A standard pitot-static tube was used for this purpose, care being taken to keep the tube alined with the stream. To determine F_θ, the direction of the stream was measured on the two sides of the screen by means of individual silk fibers from 2 to 3 inches long spaced at intervals of 1 inch on wires running parallel to the screen on both the upstream and downstream faces. For observing the upstream fibers the top of the duct was made of transparent material. The direction of the individual fibers was measured with a vernier protractor and straightedge, the protractor being read to the nearest $1/4^\circ$. Parallax was avoided by the use of a mirror on the bottom of the duct. For the evaluation of θ and ϕ the averages of the angular readings of the 10 fibers nearest the center were used. Then F_θ was calculated by equation (2).

The same procedure was repeated at various wind speeds and various angles ranging from 0° to 45°. For a given screen all measurements to determine K_θ and F_θ were made on the same sample.

The results are shown in figures 3 and 4. Figure 3, showing $K_\theta/\cos^2\theta$ plotted against $R \cos \theta$, was found to afford the best approximation to single curves for all values of θ, and therefore to represent most closely the dependence on angle. This means that the pressure drop depends on the normal component of flow through a screen even though the flow approaches with the angle θ and leaves with the angle ϕ. There was, of course, no measurement of the direction at the immediate plane of the screen.

Screens G and H were two samples from the same stock giving different results. The only known difference was that one sample was rotated in its plane 90° from the other during testing. Since this obviously cannot account for the difference in K_θ when $\theta = 0$, it is concluded that the average solidity of the two samples was different. This particular screen was not of precision manufacture, but there were no marked irregularities in wire spacing.

In figure 4, F_θ/θ is plotted against K_θ. It will be noted that there are some differences between screens but that the values for any one screen are essentially independent of θ. As shown in reference 3, a relation between F_θ/θ and K_θ is to be expected. The reasoning is as follows:

Suppose the screen to have N wires per foot, and let D be the drag of the wire forming one side of a square mesh. Further suppose the drag to be independent of the angle between the axis of the wire and the wind direction. Assume also that the induced deflection at the screen is equal to one-half the final deflection. The deflection at the screen is then given by $\delta = (\theta - \phi)/2$, and the angle at the wires is $\theta - \delta$. If the shielding of one wire by another at points of intersection is neglected, the following relations may be written:

$$ND \sin (\theta - \delta) = \tfrac{1}{2}\rho U^2 F_\theta \qquad (3)$$

$$ND \cos (\theta - \delta) + ND = \tfrac{1}{2}\rho U^2 K_\theta \qquad (4)$$

Hence

$$F_\theta = \frac{K_\theta \sin(\theta - \delta)}{1 + \cos(\theta - \delta)} \tag{5}$$

Introducing δ into equation (2),

$$F_\theta = \frac{2 \cos\theta \sin 2\delta}{\cos(\theta - 2\delta)} \tag{6}$$

By means of equations (5) and (6) it is found that there is a relation between F_θ/θ and K_θ depending somewhat on θ. If θ and ϕ are small, equations (5) and (6) reduce to

$$\frac{F_\theta}{\theta} = \frac{4K_\theta}{8 + K_\theta} \tag{7}$$

It is pointed out that equation (4) gives

$$\frac{K_\theta}{1 + \cos(\theta - \delta)} = f(R)$$

whereas figure 3 shows the more nearly correct relation to be

$$\frac{K_\theta}{\cos^2\theta} = f(R \cos\theta)$$

This means that the assumptions used in equation (4) are incorrect. Obviously they must be very crude except when the solidity approaches zero. The shortcomings of the assumptions probably become less serious as θ approaches zero; therefore, equation (7) may be fairly accurate when the solidity is low.

The curve obtained by relation (7) is shown in figure 4. Also shown in this figure is the empirical relation

$$\frac{F_\theta}{\theta} = 2 - \frac{2.2}{\sqrt{1 + K_\theta}} \tag{8}$$

obtained by Taylor and Batchelor in reference 3 on the basis of NBS data supplied to them. It is believed that equation (8) affords a reasonably accurate working formula for the range $0.7 < K_\theta < 4$.

Most of the measurements were made with one set of screen wires placed at an angle to the stream equal to the complement of θ. A few measurements made after rotating the screen in its plane through an angle of 45° showed no significant change.

When the foregoing coefficients are associated with the damping action of a screen, it is sufficient to consider limiting values as θ approaches zero, because of the fact that the flow is assumed to deviate little from normal incidence. Thus the appropriate value of K_θ is the value when $\theta = 0$, which is denoted by K. Denoting the limiting value of ϕ/θ as θ approaches zero by α, equation (2) may be written

$$\frac{F_\theta}{\theta} = 2(1 - \alpha) \tag{9}$$

By equations (8) and (9) the empirical relation between α and K becomes

$$\alpha = \frac{1.1}{\sqrt{1 + K}} \tag{10}$$

It must be remembered that the foregoing coefficients and the relations between them apply only to screens woven from round wires and having the same, or nearly the same, number of wires in two perpendicular directions.

DAMPING FORMULAS

The amount of turbulence at a given point in a stream is expressed in terms of the root-mean-square value of the velocity fluctuations at that point. It is customary to measure the longitudinal and lateral components of the fluctuations separately, these being denoted by u' and v', respectively, and the corresponding intensities by u'/U and v'/U. Thus, u'/U is a measure of the relative-speed variations, and v'/U is a measure of directional variations.

The damping produced by a screen is expressed as the ratio of the intensity found after the stream has passed through the screen to

the intensity at the same point in the absence of the screen. This ratio is called a reduction factor and is denoted by f with appropriate subscripts to distinguish between longitudinal and lateral damping. Thus:

$$f_u = (u'/U)_2/(u'/U)_1$$

$$f_v = (v'/U)_2/(v'/U)_1$$

where the subscript 2 refers to the intensity at a given point in the flow after passing through a screen, and the subscript 1 refers to the intensity at the same point with the screen absent.

When the damping of steady spatial variations is being considered, reduction factors are defined in a similar way. Let it be supposed that measurements with suitable instruments would show steady variations in speed and direction from point to point at a given section of a stream. If a screen is placed upstream from this section and the variations are reduced, the reduction factor is again the ratio of the reduced variation to the initial variation. In this case it is convenient to use the following definitions:

f_1 reduction factor for spatial variations in mean speed

f_2 reduction factor for spatial variations in mean direction

The several theoretical damping formulas for f_1, f_2, f_u, and f_v are summarized as follows. For derivations the reader is referred to the original papers.

(a) Prandtl (reference 1)

$$f_1 = \frac{1}{1 + K} \tag{11}$$

(b) Collar (reference 2)

$$f_1 = \frac{2 - K}{2 + K} \tag{12}$$

(c) Dryden and Schubauer (reference 4)

$$f_{uv} = \frac{1}{\sqrt{1 + K}} \tag{13}$$

where f_{uv} signifies that the theory does not distinguish between the damping of u' and v'. The theory is assumed to apply to the damping of turbulent energy irrespective of the distribution of this energy between longitudinal and lateral components.

(d) Taylor and Batchelor (reference 3)

$$f_1 = \frac{1 + \alpha - \alpha K}{1 + \alpha + K} \tag{14}$$

$$f_2 = \alpha \tag{15}$$

It will be noted that formula (14) reduces to formula (11) when $\alpha = 0$ and to formula (12) when $\alpha = 1$. The Prandtl and Collar formulas are thus special cases of the more general formula of Taylor and Batchelor. For screens woven from round wires such special cases are probably associated only with extremely high and extremely low solidity.

For isotropic turbulence

$$f_u^2 = \frac{(1 + \alpha - \alpha K)^2 + 2\alpha^2}{(1 + \alpha + K)^2 - 4} +$$

$$\frac{(1 + \alpha - \alpha K)^2 - 4\alpha^2}{(1 + \alpha + K)^2 - 4} \frac{3}{2}(1 - \eta^2)\left(1 + \frac{\eta^2 - \xi^2}{2\eta} \log \frac{\eta - 1}{\eta + 1}\right) \tag{16}$$

where

$$\xi^2 = \frac{(1 + \alpha - \alpha K)^2}{(1 + \alpha - \alpha K)^2 - 4\alpha^2}$$

$$\eta^2 = \frac{(1 + \alpha + K)^2}{(1 + \alpha + K)^2 - 4}$$

and

$$f_v^2 = \alpha^2 + \frac{1}{8}\left[(1 + \alpha - \alpha K)^2 - (1 + \alpha + K)^2 f_u^2\right] \qquad (17)$$

Taylor and Batchelor point out that formula (16) gives about the same numerical results as formula (14) and that the same is true of formulas (17) and (15).

The foregoing formulas apply to damping by a single screen with coefficients K and α. When several screens are used in series, and there is sufficient space between them for them to act independently, the reduction factor applies to each screen separately. However, the theory of Taylor and Batchelor leading to formulas (16) and (17) is based on isotropic turbulence approaching the screen and, according to the theory, the turbulence will not be isotropic for the second and successive screens unless there is a return to isotropy. For a theoretical treatment of the effect of more than one screen the reader is referred to reference 3.

MEASUREMENTS OF TURBULENCE AND DAMPING

The present work differed from that of 1940 in that the damping screens under investigation were placed in the 19-foot-long test section of the tunnel shown in figure 1 rather than in the settling chamber. There were at all times six damping screens in the settling chamber as permanent equipment, and it was possible to study the behavior of screens with an incident turbulence as low as 0.02 percent. Since this was much too low for damping tests, a square-mesh grid consisting of 0.2-inch-diameter rods spaced 1 inch apart was placed at the extreme upstream end of the test section. Measurements of the longitudinal and lateral components of the turbulence were made at various distances downstream from the grid through the position to be occupied by a damping screen. The measurements were made with the hot-wire turbulence-measuring equipment described in reference 6. A platinum wire 0.0002 inch in diameter and not over 0.11 inch long was used in the measurement of u', and a pair of such wires in the form of an $\times$ was used in the measurement of v'. The wire length was held down to about 0.1 inch to avoid the necessity for wire-length corrections.

The screen under test completely spanned the tunnel 120 inches from the grid, and measurements of u' and v' were repeated at various distances downstream from the screen. The result was a set of decay curves for screen absent and screen present. Three such sets

are shown in figures 5, 6, and 7. The three curves without points in each of the figures, solid upstream from the screens and broken downstream, show the turbulence for screen absent as a function of distance from the grid at three wind speeds. The solid curves with experimental points represent the measurements downstream from the screen. Sets of curves like those in figure 5 for u'/U and like those in figure 6 for v'/U were used to determine the damping of screens marked "normal" in table 1. Figure 7 is an example of "abnormal" performance.

In normal performance the turbulence resulting from the eddies shed by the screens fell off rapidly and smoothly, and there was always some low speed below which eddies ceased to form. Abnormal performance was characterized by a rise in u' with distance to high levels followed by a gradual falling off. This abnormality was always absent in v' and disappeared almost completely with low incident turbulence, as shown by the curves marked "no grid" at the bottom of figure 7. It was thought at first that this behavior was associated with high screen solidity, but this was not borne out consistently. It will be noted in table 1 that abnormality appears rather to accompany the smaller pore sizes. However, the degree of abnormality was not reproducible in different samples of the same screen and was associated, to some extent, with slight bends such as might be caused by rough handling. The 74-mesh silk bolting cloth was the worst of the lot, and here there was evidence of slight irregularities in thread spacing. It appears that nonuniformity was a contributing factor, but the nature of the effect is still unexplained. One guess is that some gross velocity pattern, either from irregularities in the screen or a coalescing of jets from the pores, is agitated laterally by the incident turbulence causing large longitudinal fluctuations.

Only screens showing normal performance could be regarded as effective dampers of turbulence, and only these were used to determine reduction factors. Even with normal performance the task of evaluating the damping was complicated by the fine-scale turbulence produced by the screen itself. However, as shown in figures 5 and 6, this turbulence disappeared when the speed was sufficiently low. On further investigation it was found that each screen had a sharply defined critical Reynolds number below which no eddies were shed. Screen turbulence could therefore be avoided by working below this critical Reynolds number. The characteristic behavior of a screen above and below the critical Reynolds number is shown in figure 8. There were, however, two difficulties at low speeds that made it advisable not to depend solely on the measurements below the critical Reynolds number. There was first a marked Reynolds number effect on the grid, causing the turbulence incident to the screen to decrease sharply as the speed decreased; and, second, the determination of screen parameters was less certain at the lower speeds.

Reduction factors were therefore determined both above and below the critical Reynolds number. In both cases it was desired to obtain the reduction resulting from the screen, not that resulting from decay. Measurements showed that the influence of the screen began from 1/2 to 1 inch upstream. Since only about one-half of the final reduction was observed on the upstream side, the effect probably extended about the same distance downstream; but direct observation of the extent was impossible because of interference from the wakes of the wires of the screen. Below the critical Reynolds number, reduction factors could be determined by comparing the measured turbulence just beyond the zone of influence with that existing in the absence of the screen at the same point. Above the critical Reynolds number the turbulence coming through was mixed with screen turbulence, and the procedure adopted to obtain the appropriate value near the screen was to use the decay law that would exist in the absence of screen turbulence to extrapolate back to the screen from some point far out on the curve. This involved a knowledge of the scale of the turbulence and the assumption that some portion of the curve far from the screen was essentially unaffected by screen turbulence. By regarding a screen as a grid it was fairly evident that the assumption was valid beyond 40 inches for all of the screens. Scale measurements verifying this assumption are discussed in the next section.

The reduction factors so determined are shown in figures 9 and 10. The theoretical reduction factors given by formulas (13), (16), and (17) are shown by the curves, with equation (10) furnishing the relation between α and K. By referring the position of the points to the curve common to both figures, namely the $1/\sqrt{1 + K}$-curve, it will be seen that the difference between the reduction in u'/U and v'/U is scarcely outside the experimental scatter. It is evident that $1/\sqrt{1 + K}$ is in better agreement with the observed reduction factors for u'/U than formula (16). As for the lateral component shown in figure 10, it is difficult to make a distinction between the agreement for the two theories. The points connected by arrows show the trends with increasing Reynolds number occurring in all cases when observations were taken at different Reynolds numbers from well below up to the critical value. No such trends were noted above the critical Reynolds number.

The general conclusion to be drawn from the foregoing results is that the simple damping law $1/\sqrt{1 + K}$ stands in best over-all agreement with the observations. This confirms the results of the 1940 work given in reference 4. However, the derivation of this law involves assumptions that now seem unjustifiable. For example, it must be assumed that all of the reduction takes place on the upstream side of the screen. Measurements upstream from a screen showed that about one-half of the reduction takes place there. Furthermore, it is difficult to see how the law can apply to v'. It now appears that

the effect on v' is more logically given by the Taylor-Batchelor law, equation (17), and only happens to agree with the $1/\sqrt{1 + K}$-law because of the relation $\alpha = 1.1/\sqrt{1 + K}$ (equation (10)).

EFFECT OF SCREENS ON SCALE

One of the commonly used scales is known as the integral scale, defined by

$$L_y = \int_0^\infty R_y \, dy$$

where

$$R_y = \frac{\overline{u_1 u_2}}{u_1' u_2'}$$

$\overline{u_1 u_2}$ being the mean product of the longitudinal fluctuations at points 1 and 2 separated by a lateral distance y, and u_1' and u_2' being the root-mean-square values of u_1 and u_2. In the decay of isotropic turbulence there is an increase in scale accompanying the decrease in intensity. To determine whether there was also a change in scale when turbulence was damped by a screen, R_y was measured as a function of y at a distance of 3 inches downstream from each of two different screens below the critical Reynolds number and again without screens at two wind speeds. The results are shown in figure 11. Clearly there was no effect big enough to be detected. The scale L_y remained equal to 0.41 inch in all cases, even though the intensity was reduced by a factor of 0.45 in one case.

When the velocity was increased to exceed the critical Reynolds number, the scale became very small indicating the presence of small-scale turbulence from the screen. However, measurements made at a distance of 47 inches from the screens showed that the scale had returned to its original value.

The absence of change in L_y means that damping has reduced the energy of all frequencies of the u-component of the turbulence by the same factor. This follows from the known relation between scale and

spectrum in isotropic turbulence (reference 7). However, the scale does not afford a sensitive test, and the present result should be regarded only as a qualitative indication that damping is not selective of any particular frequency.

CRITICAL REYNOLDS NUMBER AND PRODUCTION OF EDDIES

By placing a very short hot wire (length about 0.05 in.) within 1 inch of a screen it was easy to observe the periodic shedding of eddies from a screen. When the incident turbulence was down to a few hundredths of 1 percent, the eddies produced an almost purely sinusoidal wave on the screen of a cathode-ray oscillograph. Under these conditions the critical Reynolds number for the beginning of eddy shedding could be determined with high accuracy by slowly raising the airspeed and observing the sudden appearance of eddies. After the initial appearance of eddies, it was possible to observe a definite frequency related to the speed. For certain lateral positions of the wire it was possible to find half or double this frequency, but there was always one most prominent frequency. This is given in figure 12 in terms of the frequency number nd/U where n is frequency in cycles per second. The numbers on each curve represent the solidity of the screen. Each curve begins at the critical Reynolds number and ends where distortion of the pattern prevented accurate measurement of frequency.

The critical Reynolds numbers were found to be a function of the solidity as shown in figure 13. These were shown also to be the Reynolds numbers for the initial production of turbulence by observing the initial increase in u' at distances of 100 mesh lengths or more downstream. It was found in addition that the critical Reynolds numbers were unchanged when the incident turbulence was raised to the level used in damping measurements. The mean values of the critical Reynolds number found for each screen and the corresponding critical speeds are given in table 2.

There appears to be no connection between these results and those for a single cylinder, nor is there any apparent trend toward the characteristics of a single cylinder with decreasing solidity. It appears therefore that a woven square mesh of wires has unique characteristics determined by its configuration.

DAMPING OF MEAN-SPEED VARIATIONS

Investigations of the damping of steady spatial speed variations were made by Collar (reference 2) and MacPhail (reference 8), and both concluded fair agreement with formula (12). Taylor and Batchelor, using these same experimental results, found better agreement with formula (14).

In considering a reinvestigation of this problem, it was noted that both Collar and MacPhail dealt with the large speed variations found in the wakes of flat strips and corner vanes, and these appeared to be rather large to test theories in which the disturbances were assumed to be small. Accordingly, an effort was made to set up smaller variations and to try different amplitudes and different lateral distributions. For this purpose screens were made up with strips of alternate high and low solidity, as indicated by figure 2(b). These were placed in test apparatus B at section B (fig. 2(d)), and the assembly was connected to the blower and duct system. Four such screens were used to obtain four different distributions, three of the screens having strips 1 inch wide and the fourth having strips 3 inches wide.

The test procedure was to determine the flow distributions by traversing in planes perpendicular to the strips at various distances downstream with a small pitot-static tube. This tube read dynamic pressure to within 2 percent up to angles of attack of 20°. The damping screen to be tested was then placed to span the duct at section A (fig. 2(d)), 9 inches downstream from the nonuniform screen, and the flow distributions were again determined. Samples of the distributions are shown in figure 14. On the graphs of figure 14 solid lines represent the data taken without the damping screens, and the plotted points indicate the distributions after the damping screen was placed in position. All measurements were made at a mean speed of 25 feet per second.

The amplitude was defined as the average deviation from $U/\bar{U} = 1$ and was determined in all cases by finding areas under a representative number of loops near the stream center line, both above and below the mean-velocity line, and dividing by the same number of half wave lengths. In cases when the amplitude was small or the K-value of the screen was large, random irregularities superposed upon the basic wave gave rise to difficulties in determining amplitude. There were in fact some cases where no trace of the original wave could be found by inspection, yet by measuring areas for intervals corresponding to half wave lengths it was possible in most cases to find the remnant of the original wave. There was evidence that some of the random variations may have been introduced by the damping screen. However, the method

of finding amplitudes should eliminate all but the component of random variations having the same wave length as the basic wave, and the error from random variations should be small.

The amplitudes, in percentage of mean velocity, are plotted in figure 15 as a function of distance from the source. The curves which are drawn as solid lines upstream from the damping screen and continued as broken lines downstream show the decay with damping screen absent. All other curves show the amplitudes with the damping screen present.

The purpose of these and similar curves was to eliminate the natural decay in finding the reduction produced by the damping screen. In doing this a region of influence of the screen had to be taken into account. Figure 15(d) shows how the screen reduces amplitudes upstream and continues to do so downstream. The region through which the influence of the screen was felt extended both upstream and downstream for a distance of about 1 wave length. Within this region, silk-fiber direction indicators showed the high-velocity portions of the stream to be fanning out. Also within this region, and only within this region, the static pressure was found to be above average in regions of high velocity and below average in regions of low velocity on the upstream side of the screen, and the reverse on the downstream side. These phenomena are evidence of a diffusing action not unlike that shown for screens in diffusers in reference 9.

Recognizing that the effect of a screen is not confined to its plane, the procedure adopted was to determine a curve of natural decay from a composite plot of all decay curves. This curve was then used to extrapolate the individual curves, as illustrated by the broken lines branching from the solid lines back to the plane of the screen in figure 15(d). The reduction by the screen was then regarded to be the step-down at the screen from the uppermost broken curve (screen absent) to any one of the lower broken curves.

The reduction factors so determined are shown plotted in figure 16 along with the theoretical curves of Prandtl, Collar, and Taylor and Batchelor, equation (10) being used to express α in terms of K. The possibility of error caused by random variations is greater for high values of K than for low values and also greater for the lower amplitudes, such as distribution III, than for the others. Regardless of possible errors in magnitude, the values at $K = 3.7$ are definitely negative. On the whole, the experiment is believed to confirm the Taylor-Batchelor theory about as well as can be expected.

It may be noted that no points are given for K above 3.7. The reason for this is that the random speed variations put in by the damping screen itself became too troublesome at the higher values. Screen J, having values of K from 11 to 19, put in random variations

so much larger than those upstream that it was much better as a producer of disturbances than as a damper. Far downstream from screens with a K-value above 3.7 the random variations gave way to a region of high velocity in the central portion of the stream.

CONCLUSIONS

From an investigation of the effects of damping screens and their performance in oblique flow, the following conclusions were drawn:

1. A sufficient amount of information was obtained on normal- and tangential-force coefficients of square-mesh screens woven from round wires to predict pressure drop and stream deflection for angles of incidence up to 45° and solidities up to 0.79. It is believed that this information will be useful, not only for damping applications, but for other applications as well.

2. When a stream approaches a screen with the velocity U at the angle θ and leaves at the angle ϕ, the pressure drop is a function of $U \cos \theta$. In other words, the pressure drop under these conditions is determined by the normal component of the approach velocity. No information was obtained for θ greater than 45°.

3. The damping results, which are in general agreement with those obtained in 1940, show that a screen reduces u' and v' (root-mean-square values of longitudinal and lateral turbulence fluctuations, respectively) by closely the same factor and that this factor is given by $1/\sqrt{1 + K}$ (K being the pressure-drop coefficient when $\theta = 0$) when the Reynolds number of the screen is equal to, or above, the critical value for the initial shedding of eddies by the screen. Below the critical Reynolds number the factor becomes progressively less (greater reduction) as the Reynolds number is reduced.

4. The reduction factor for v' should logically obey the Taylor-Batchelor law, and probably only appears to be given by $1/\sqrt{1 + K}$ because $\alpha = 1.1/\sqrt{1 + K}$.

5. The scale of turbulence is unchanged by a damping screen.

6. Every screen has a well-defined Reynolds number above which eddies are shed. This Reynolds number depends on the solidity of the screen.

7. The eddies produced by a damping screen result in turbulence of small scale which decays rapidly in the first few feet. However, the rate of decay becomes low at a turbulence level around 0.1 percent, and long distances are required if the screen itself is not to set a lower limit of the order of 0.1 percent. Obviously, a screen should be followed by a contraction of the stream to increase the mean speed and so decrease the percentage value of the turbulence. Whenever possible the cross section of the stream at the screen should be sufficiently large to operate the screen below the critical Reynolds number. This would appear especially desirable in small wind tunnels where distances for decay are small.

8. Under certain conditions, which are not completely understood, a screen may produce abnormally high and slowly decaying longitudinal fluctuations. This condition must be avoided if the screen is to be an effective damper of turbulence.

9. As a general observation, based on the performance of damping screens throughout these experiments, screens of high K are less satisfactory as dampers than screens of low K. This applies both to turbulence and spatial variations. As also observed in previous studies, it appears preferable to obtain a given reduction by using several screens of low K in series rather than by using a single screen of high K.

10. The observed damping of steady spatial variations tends to confirm the Taylor-Batchelor theory and is in better agreement with that theory than is the observed damping of turbulence.

National Bureau of Standards
Washington, D. C., January 28, 1949

REFERENCES

1. Prandtl, L.: Attaining a Steady Air Stream in Wind Tunnels. NACA TM 726, 1933.

2. Collar, A. R.: The Effect of a Gauze on the Velocity Distribution in a Uniform Duct. R. & M. No. 1867, British A.R.C., 1939.

3. Taylor, G. I., and Batchelor, G. K.: The Effect of Wire Gauze on Small Disturbances in a Uniform Stream. Quart. Jour. Mech. and Appl. Math., vol. II, pt. 1, March 1949, pp. 1-29.

4. Dryden, Hugh L., and Schubauer, G. B.: The Use of Damping Screens for the Reduction of Wind-Tunnel Turbulence. Jour. Aero. Sci., vol. 14, no. 4, April 1947, pp. 221-228.

5. Simmons, L. F. G., and Cowdrey, C. F.: Measurements of the Aerodynamic Forces Acting on Porous Screens. R. & M. No. 2276, British A.R.C., 1945.

6. Schubauer, Galen B., and Skramstad, Harold K.: Laminar Boundary-Layer Oscillations and Transition on a Flat Plate. Jour. Res. Nat. Bur. of Standards, Res. Paper RP1772, vol. 38, no. 2, Feb. 1947, pp. 251-292; also NACA Rep. 909, 1948.

7. Dryden, Hugh L.: A Review of the Statistical Theory of Turbulence. Quart. Appl. Math., vol. 1, no. 1, April 1943, pp. 7-42.

8. MacPhail, D. C.: Experiments of Turning Vanes at an Expansion. R. & M. No. 1876, British A.R.C., 1939.

9. Schubauer, G. B., and Spangenberg, W. G.: Effect of Screens in Wide-Angle Diffusers. NACA TN 1610, 1948.

TABLE 1.- SCREENS

Screen designation	Wires per inch	Wire diameter (in.)	Pore size (in.)	Solidity	Performance in turbulence test
A[a]	4	0.025	0.225	0.190	Normal
B	24	.0075	.0342	.328	Do.
C	20	.0170	.0330	.564	Do.
D	40	.007	.0180	.481	Do.
E	50	.0055	.0145	.474	Abnormal
F	54	.0055	.0130	.506	Do.
G	50 by 60	.007	.0130 by .0097	.623	Not used
H	50 by 60	.007	.0130 by .0097	.623	Do.
J	40	.0135	.0115	.788	Do.
K[b]	74	[c].005	.0085	.603	Abnormal

[a]Damping results not included.
[b]Silk cloth manufactured for bolting flour.
[c]Thread.

TABLE 2.- MEAN CRITICAL REYNOLDS NUMBERS AND CORRESPONDING CRITICAL SPEEDS

Screen designation	Wires per inch	Critical Reynolds numbers	Critical speed[1] (fps)
A	4	66	4.8
B	24	55	13.2
C	20	32.5	3.4
D	40	46	11.9
E	50	46	15.1
F	54	44	14.4

[1]For air at 15° C, 760 mm Hg.

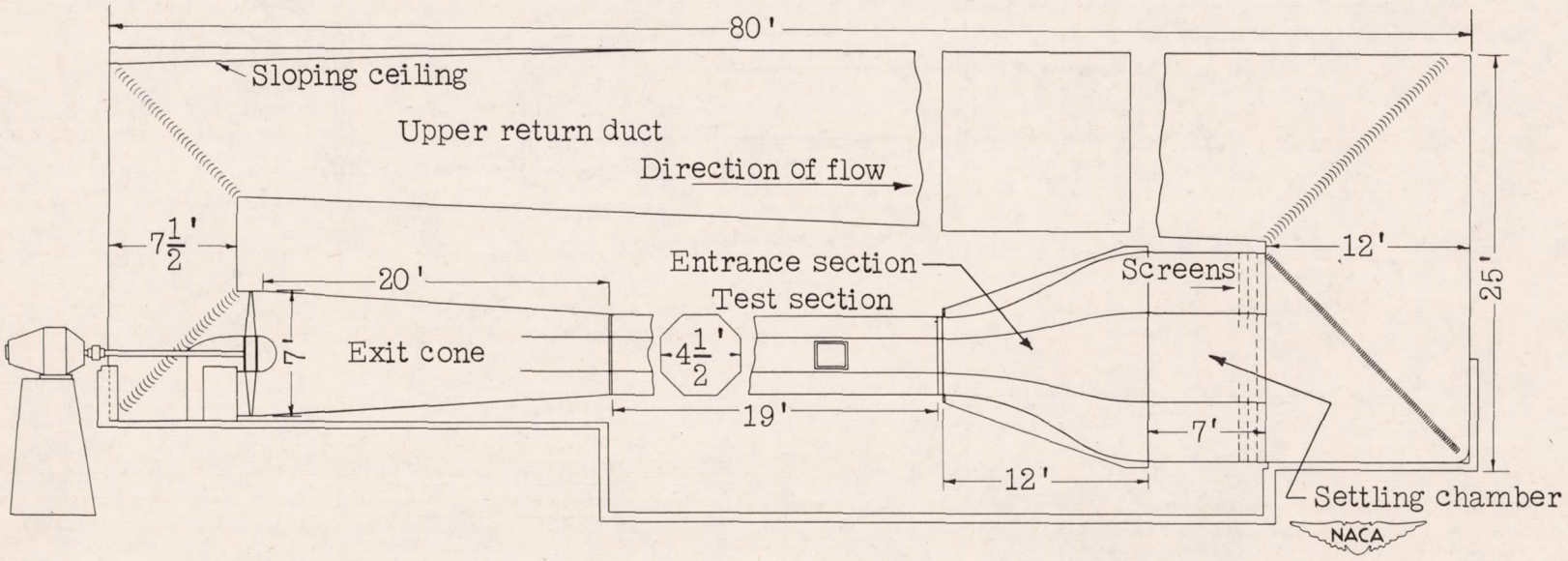

Figure 1.- Elevation view of $4\frac{1}{2}$-foot wind tunnel.

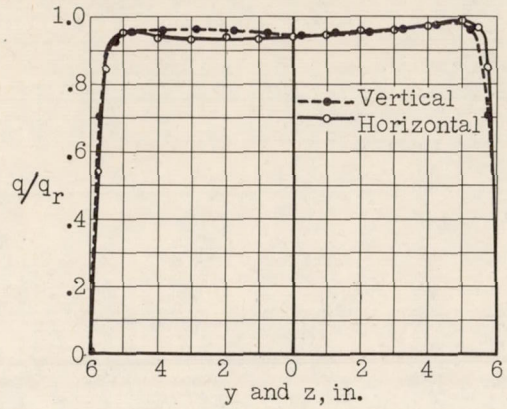

(a) Traverses at section C. q, dynamic pressure; q_r, reference dynamic pressure; y and z, horizontal and vertical distances, respectively.

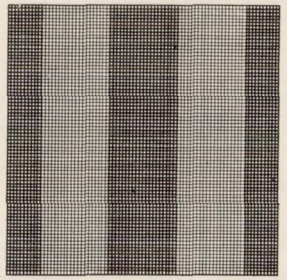

(b) Nonuniform screen used at section B of test apparatus B.

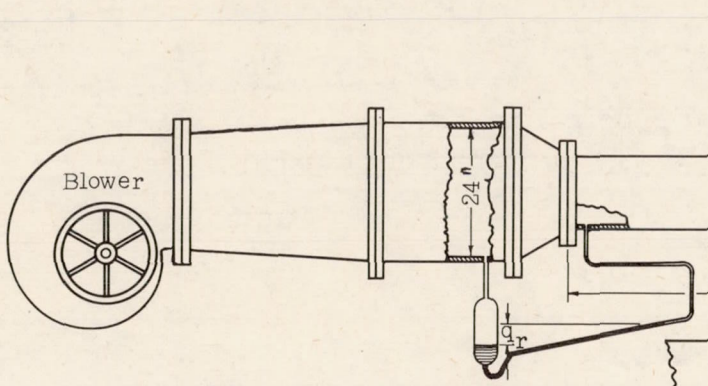

(c) Test apparatus A. p, static pressure before screen; p_2, static pressure after screen; $\overline{U}_2$, mean velocity after screen.

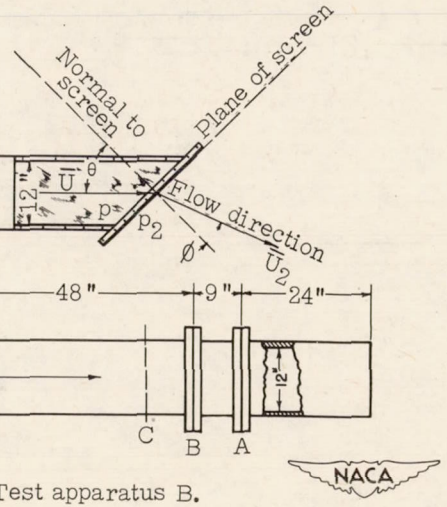

(d) Test apparatus B.

Figure 2.- Apparatus used in determining coefficients of screens and damping of spatial variations in speed.

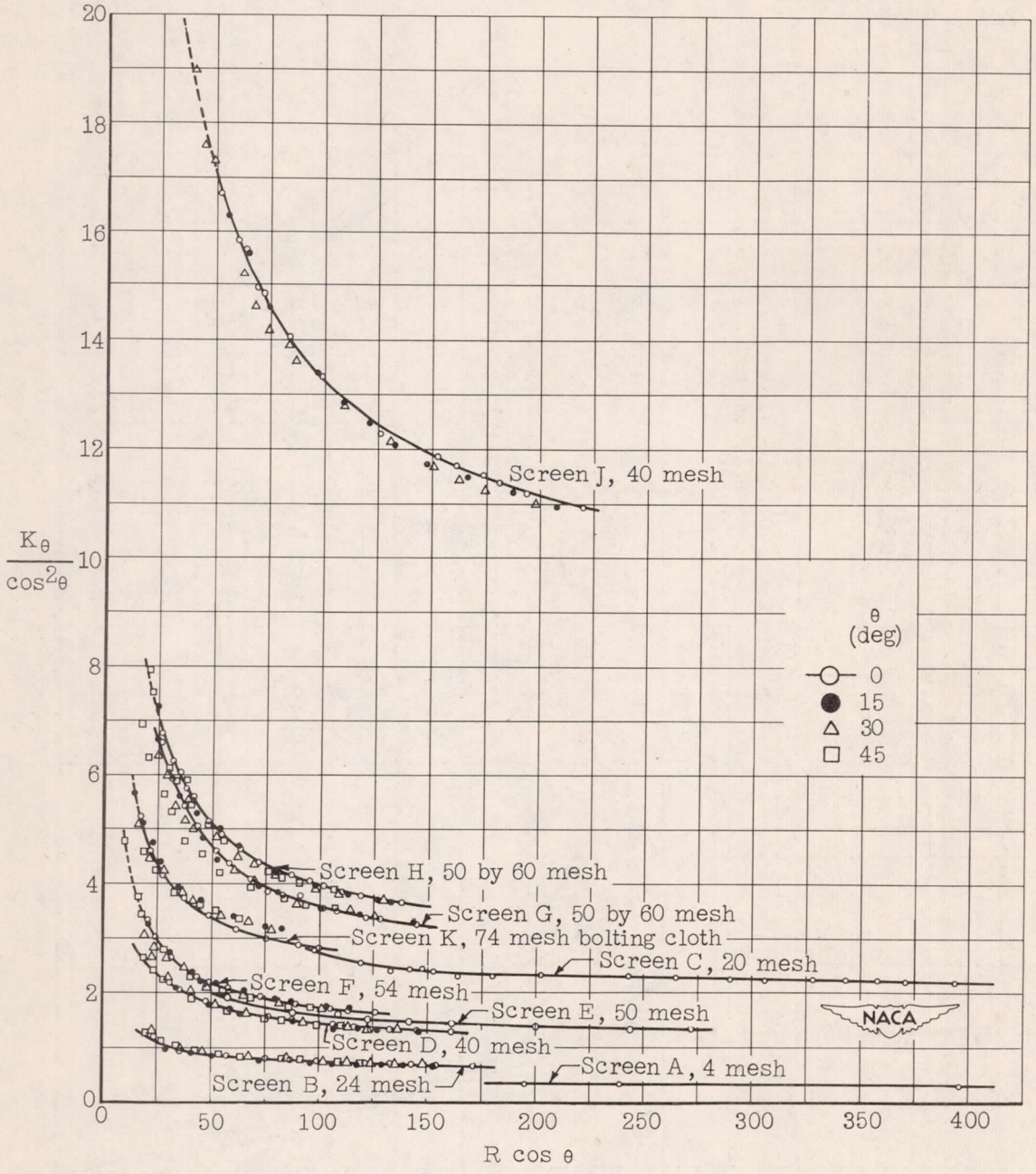

Figure 3.- Pressure-drop coefficients for flow incident at angle θ and freely deflected by screen. All curves are drawn for $\theta = 0^\circ$.

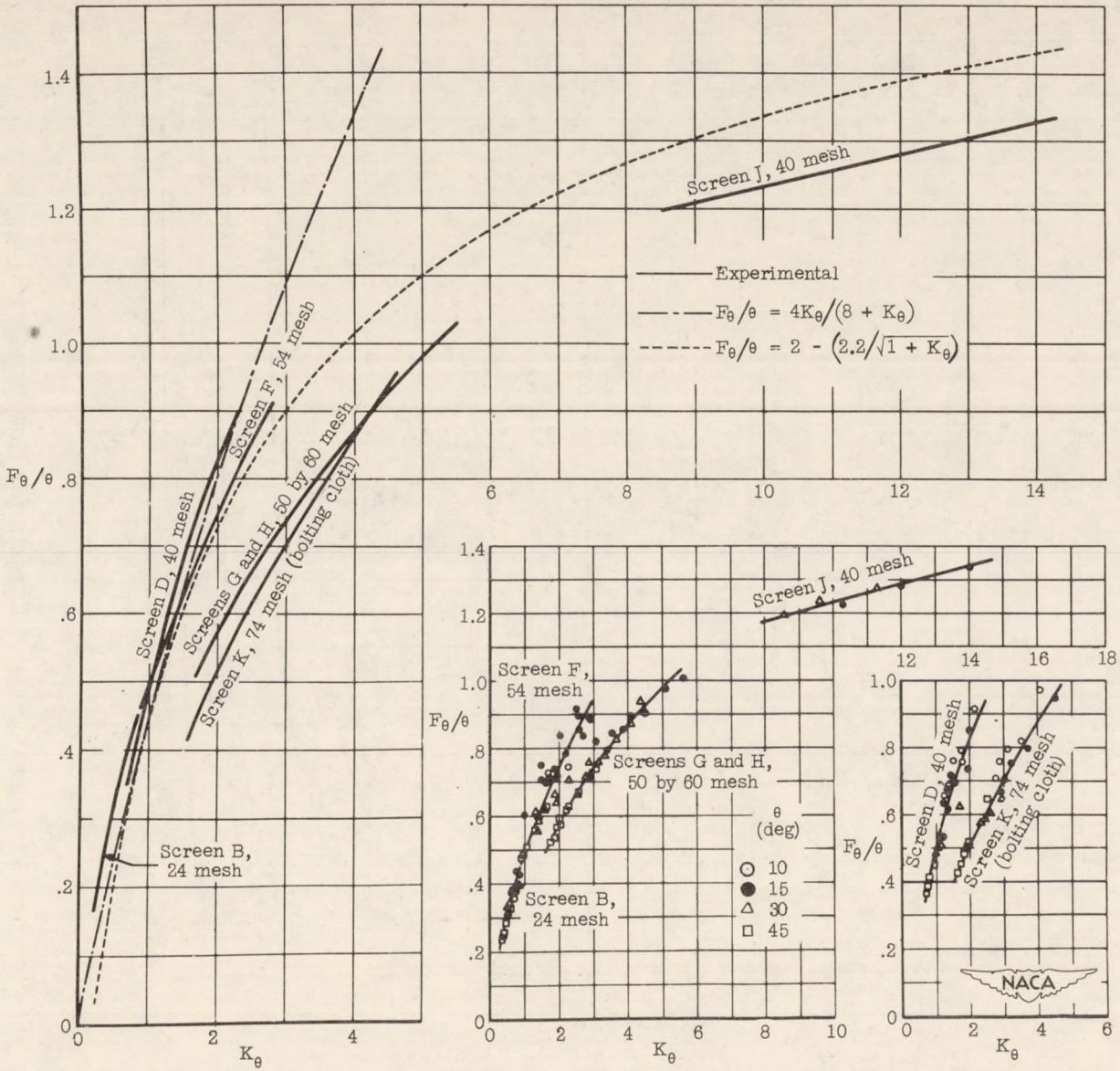

Figure 4.- Curves showing tangential-force coefficient as a function of pressure-drop coefficient.

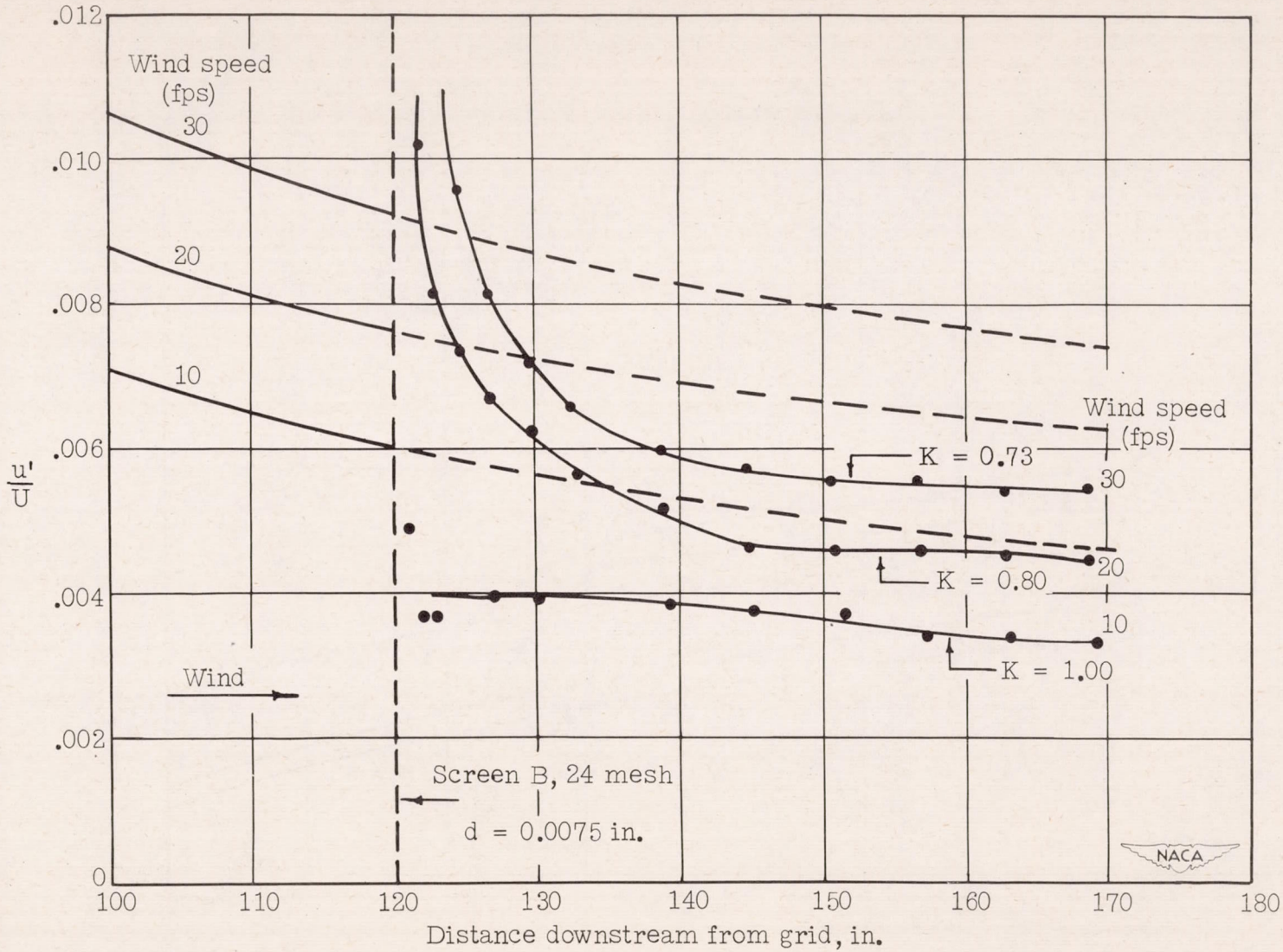

Figure 5.- Longitudinal component of turbulence. Curves without points for screen absent.

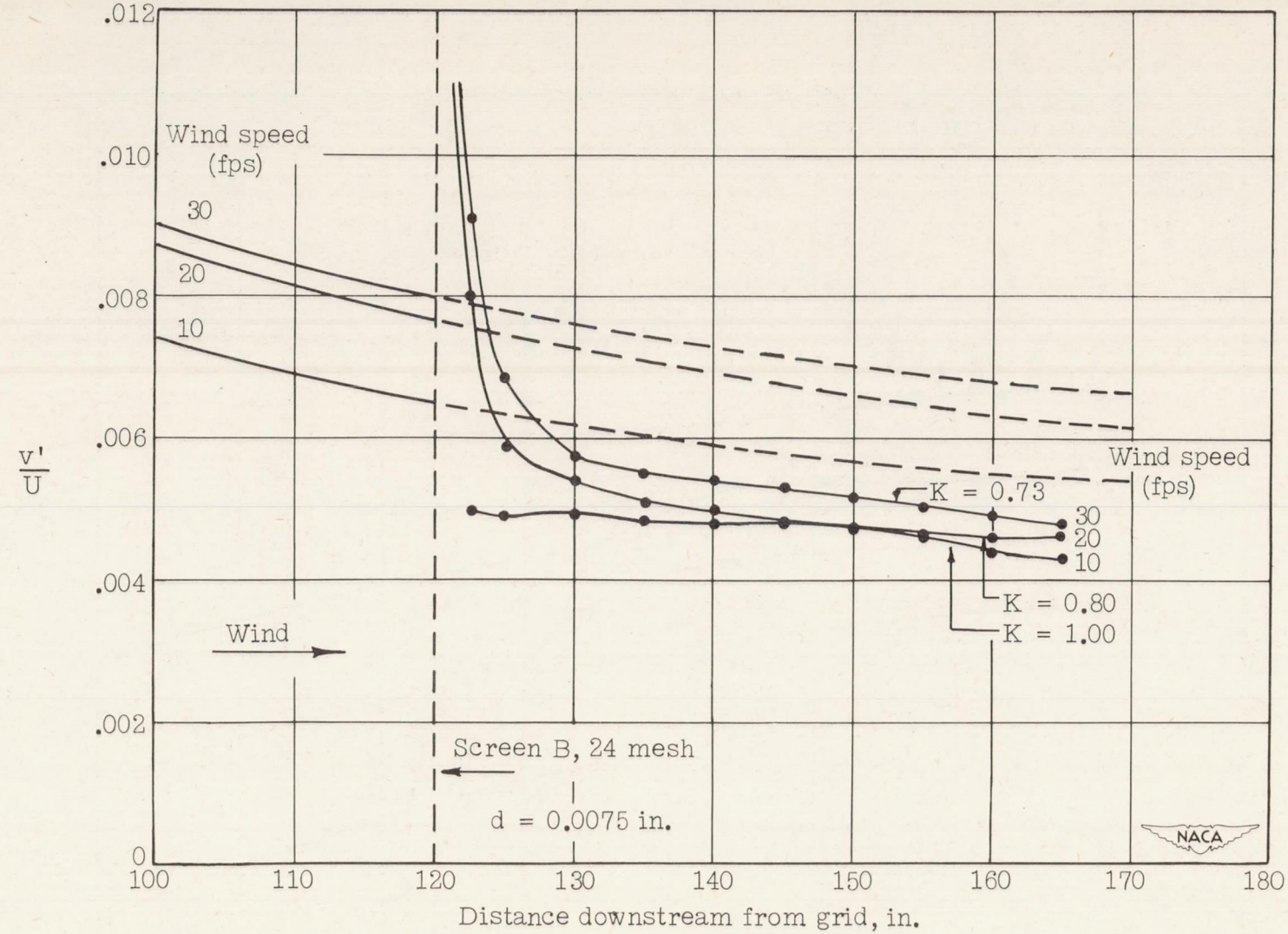

Figure 6.- Lateral component of turbulence. Curves without points for screen absent.

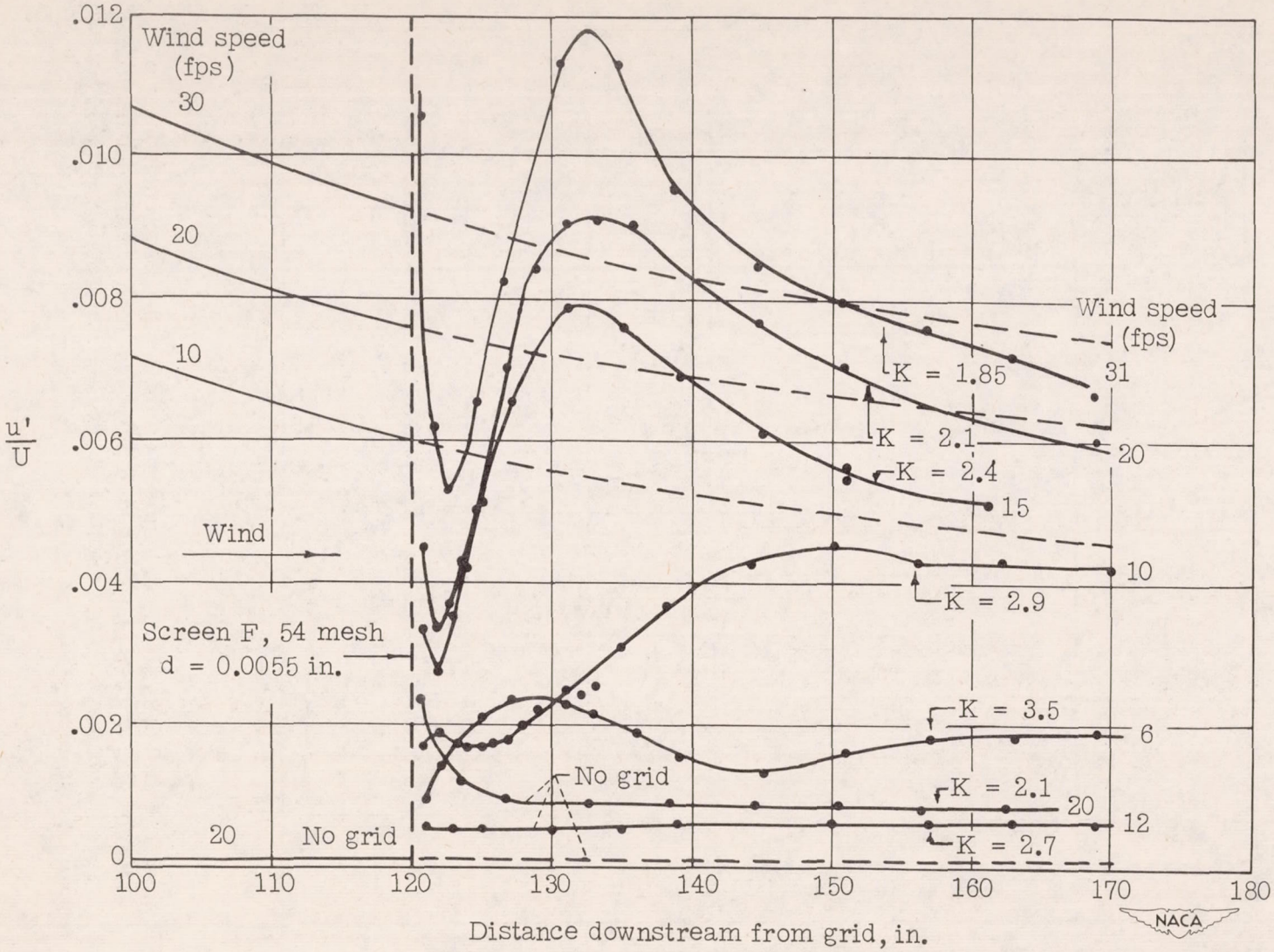

Figure 7.- Longitudinal component of turbulence showing abnormal performance. Curves without points for screen absent.

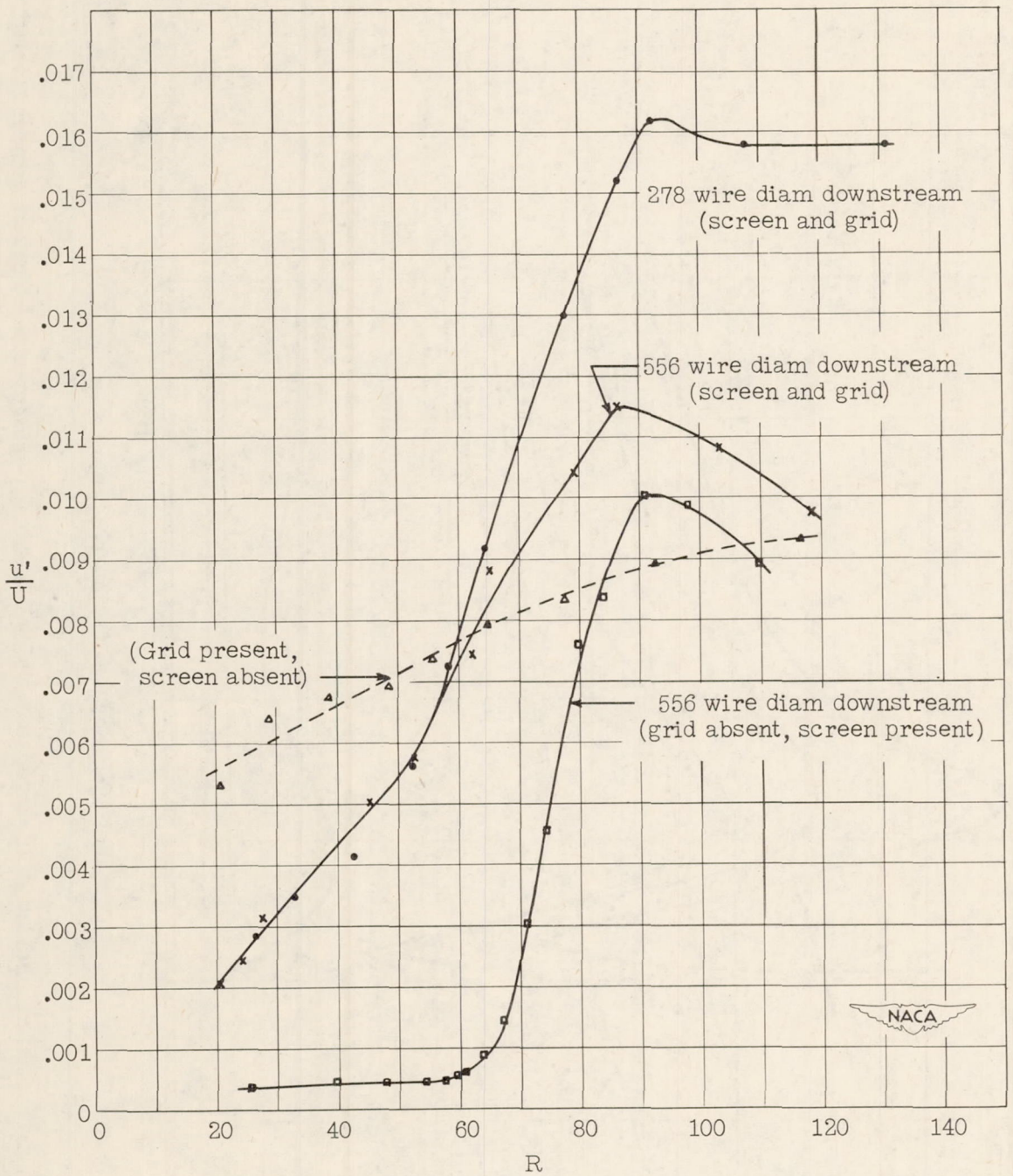

Figure 8.- Effect of Reynolds number on the longitudinal component of turbulence. Curves show the scale effect on grid and the dependence of screen turbulence on the critical Reynolds number. Screen B, 24 mesh; d = 0.0075 inch.

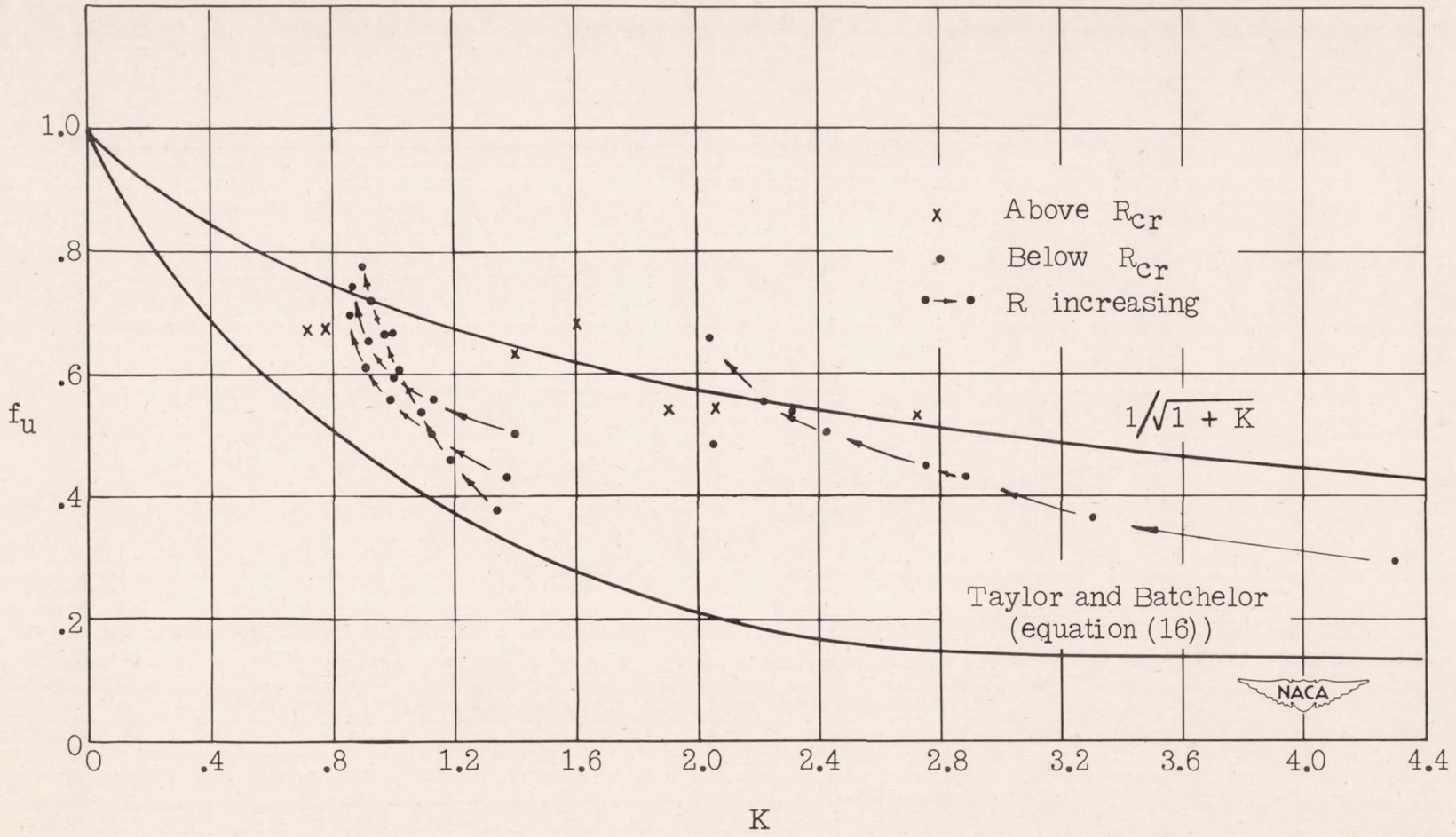

Figure 9.- Reduction factors for longitudinal component of turbulence. R_{cr}, critical Reynolds number.

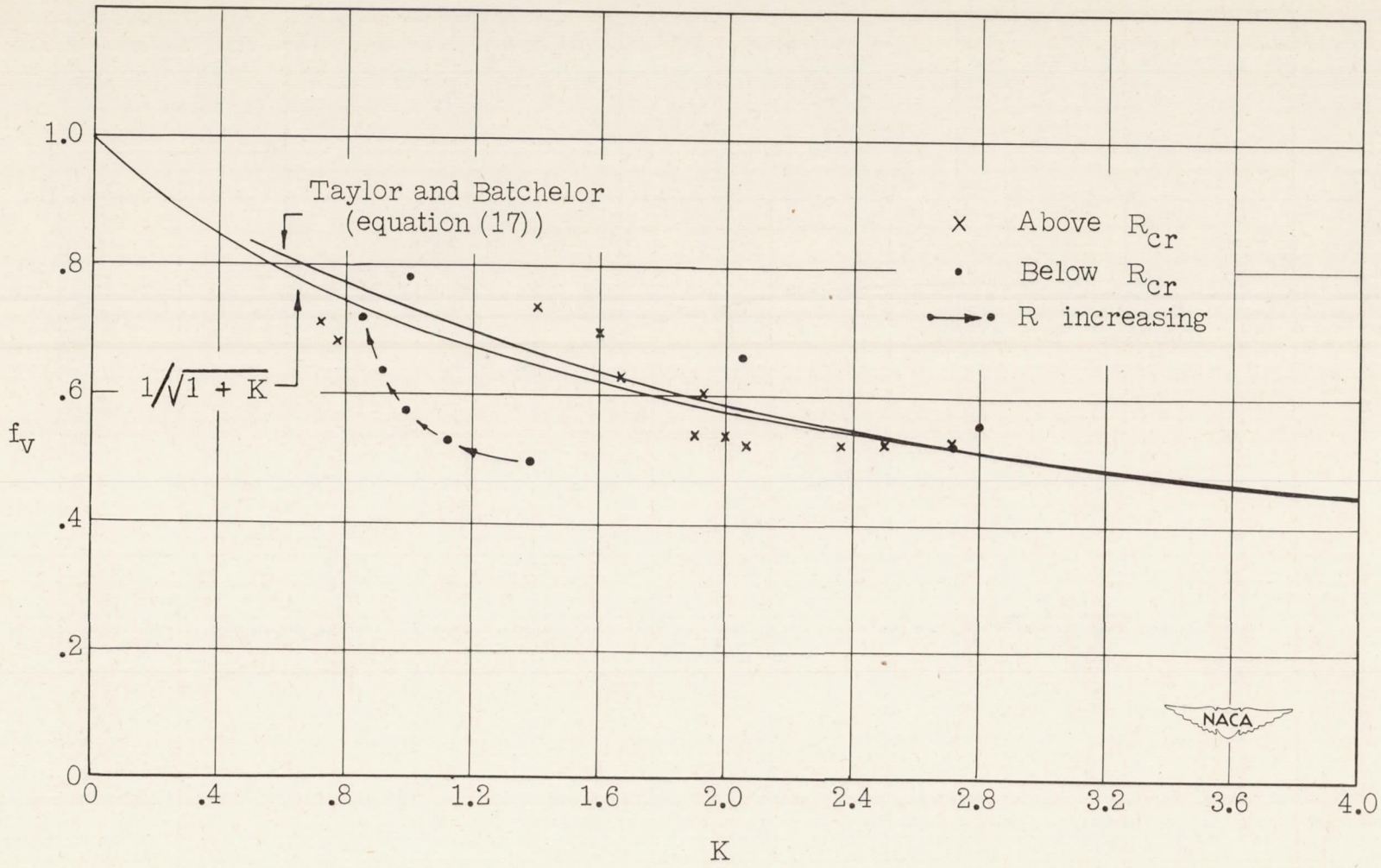

Figure 10.- Reduction factors for lateral component of turbulence.

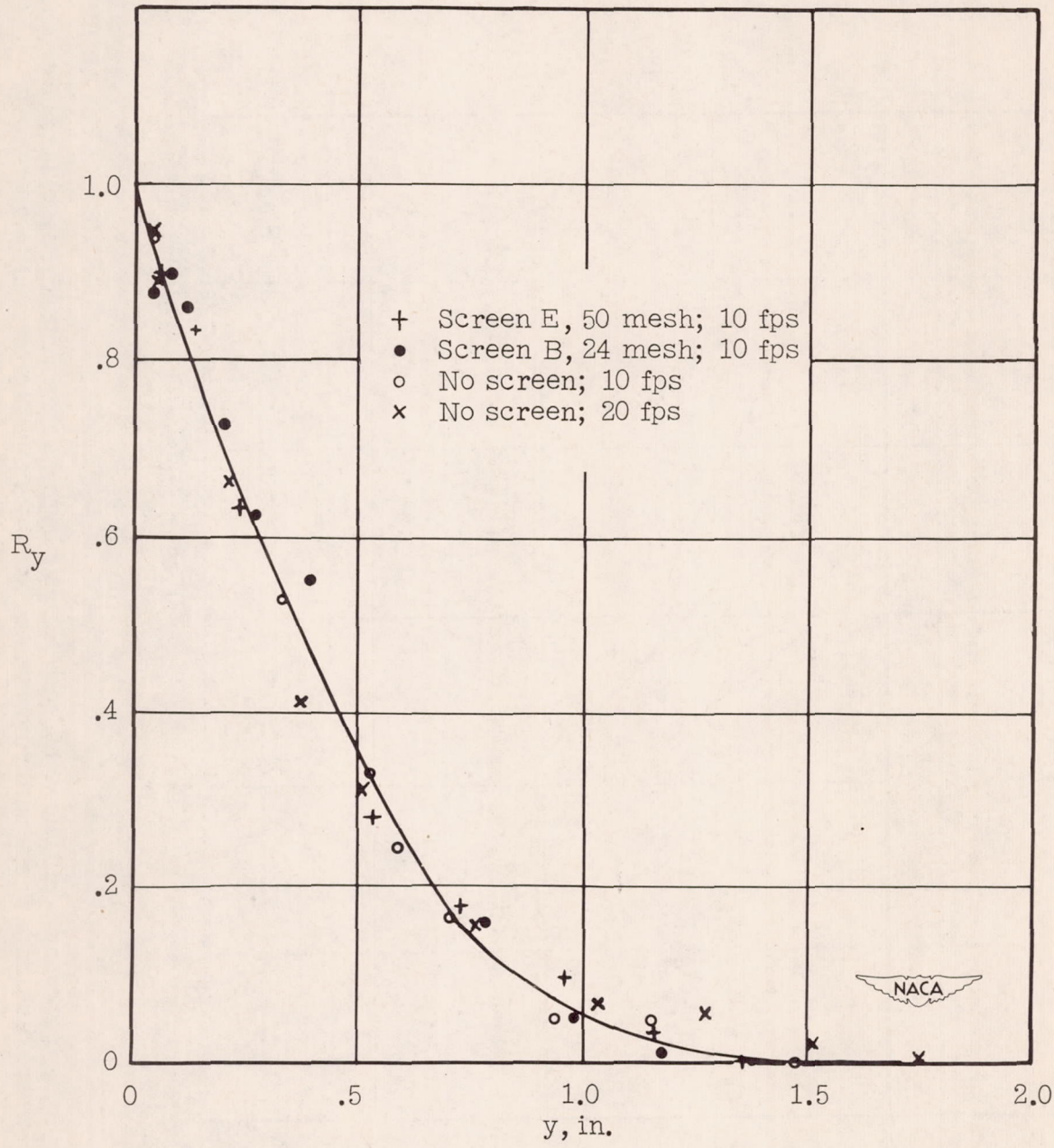

Figure 11.- Correlation coefficient and lateral scale. Measurements made 3 inches downstream from position of screens. L_y = 0.41 inch.

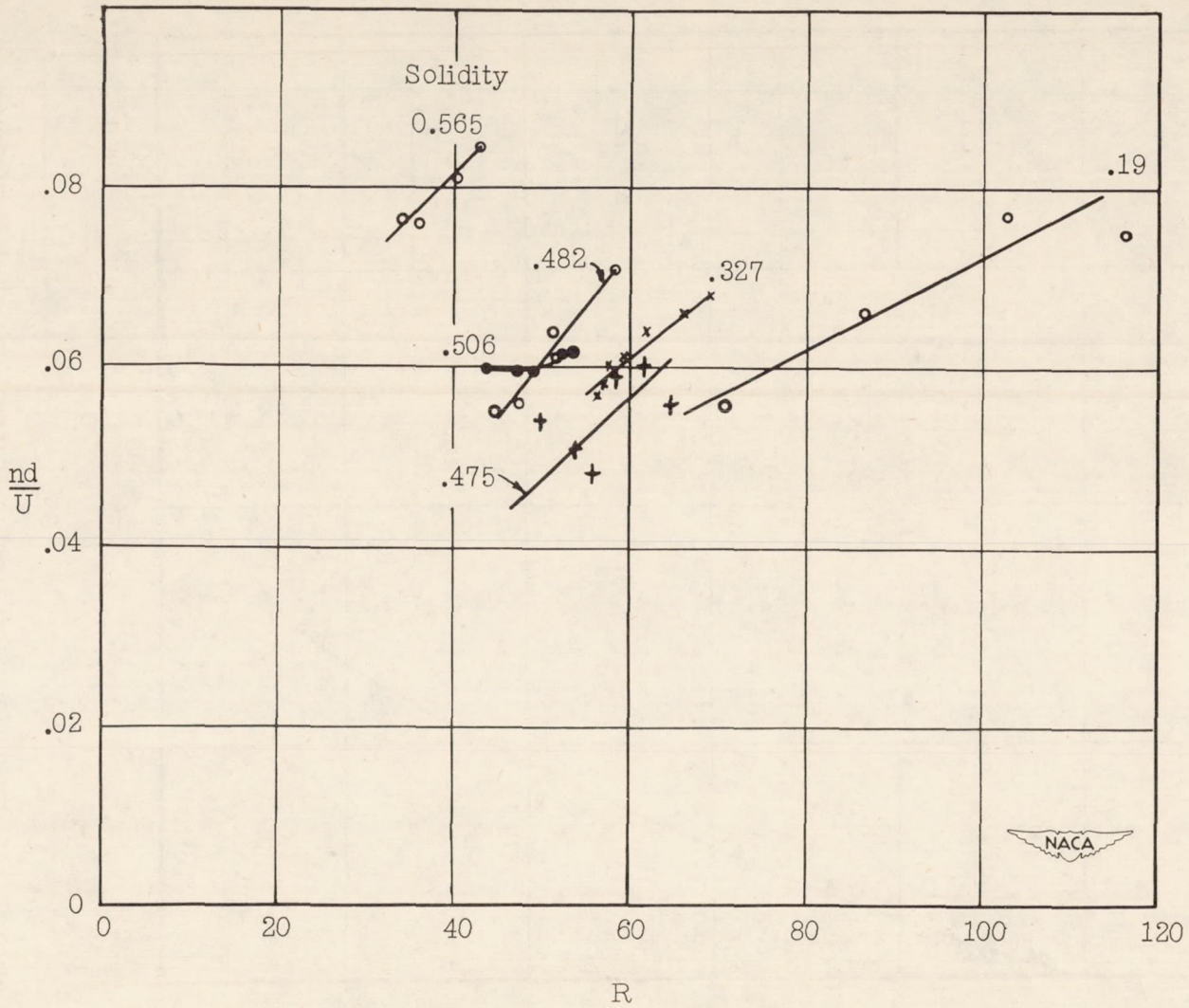

Figure 12.- Eddy frequency behind screens. Each curve begins at the critical Reynolds number and ends where distortion of the pattern prevented accurate measurement of frequency.

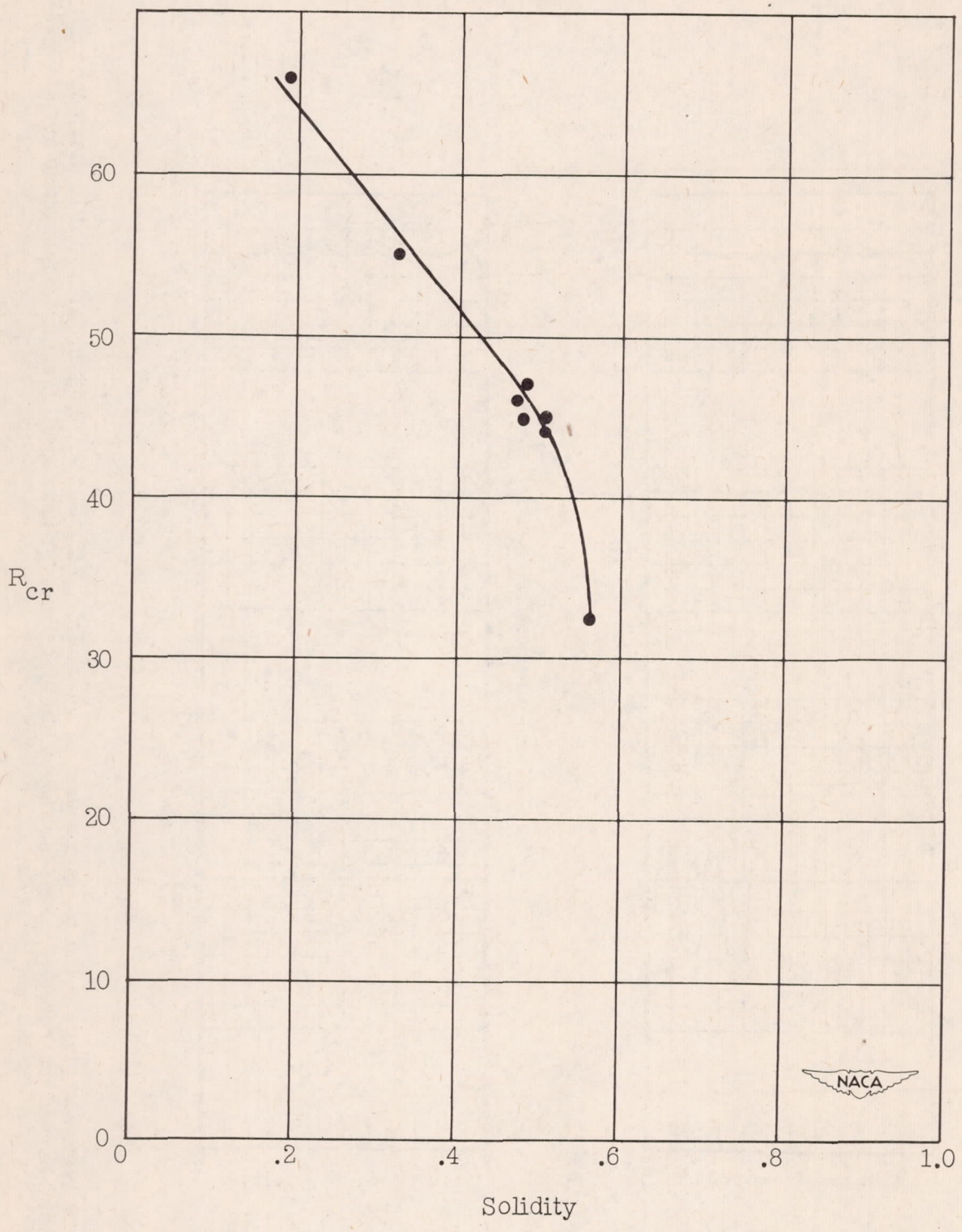

Figure 13.- Critical Reynolds number above which eddies are produced, showing dependence on solidity of screen.

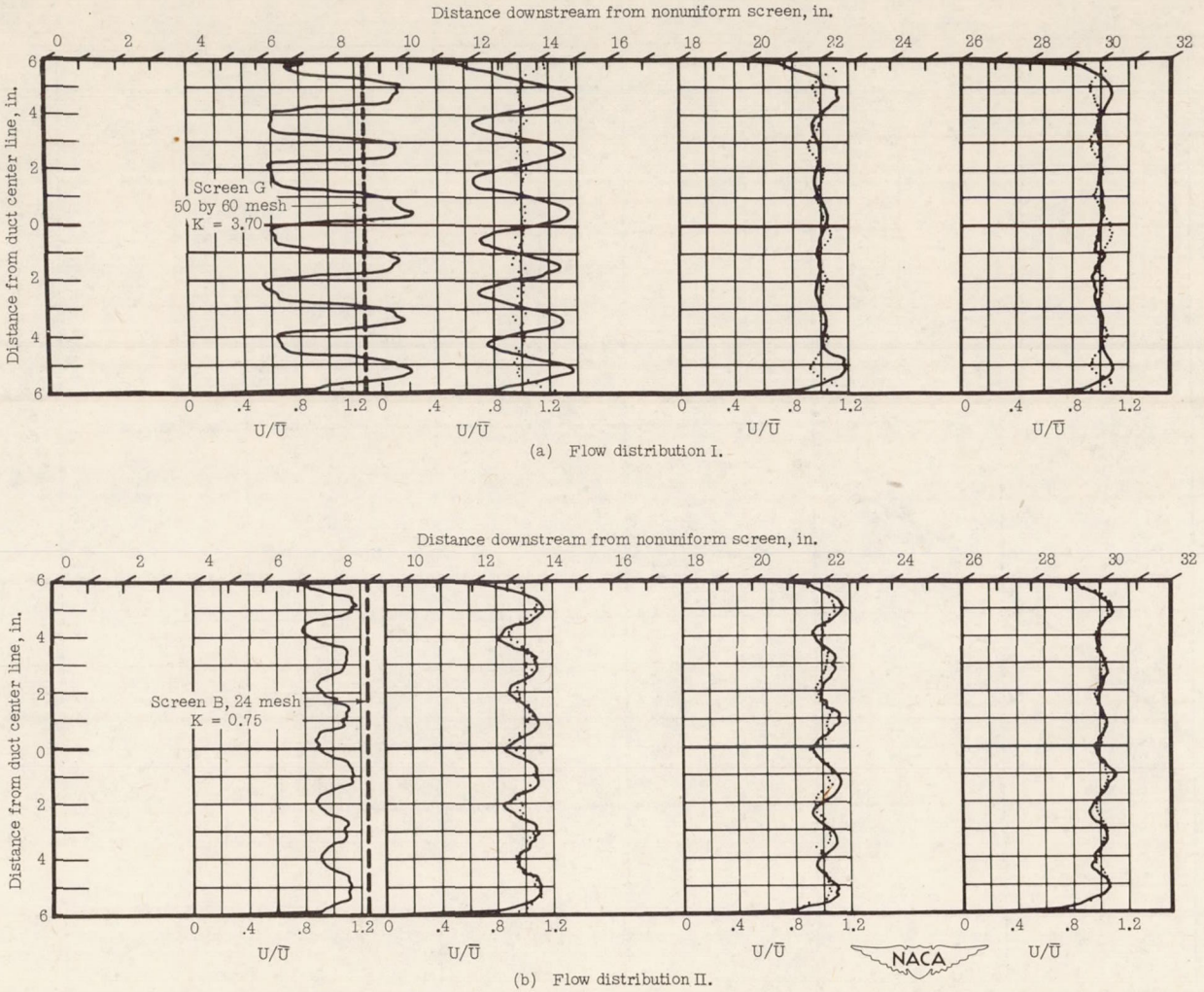

Figure 14.- Sample flow distributions used in determining effect of screens on variations in mean speed. Solid curves for screen absent; plotted points for screen present. All measurements made at $\overline{U}$ = 25 feet per second.

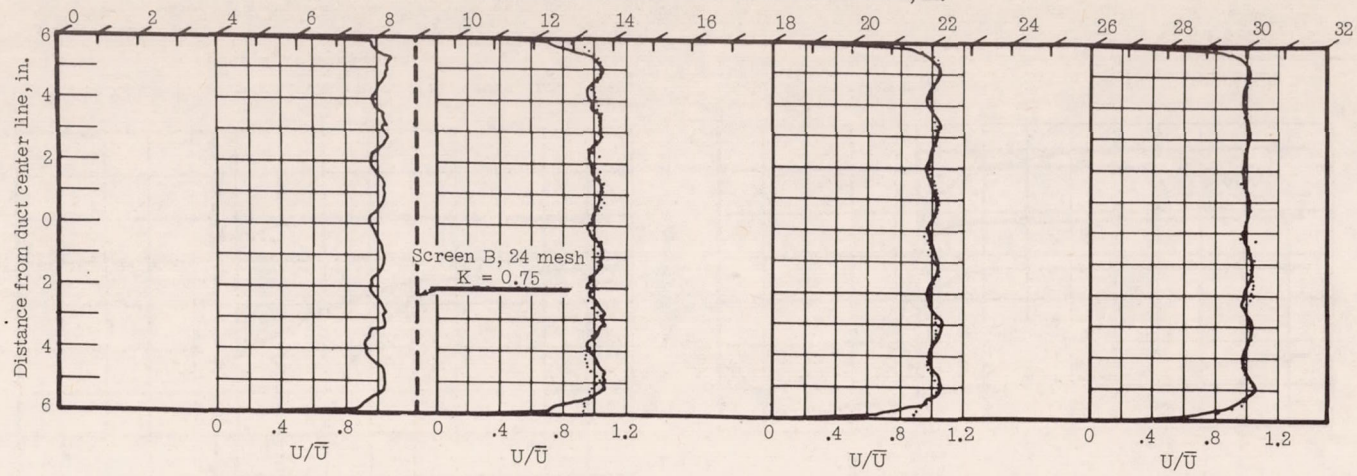

(c) Flow distribution III.

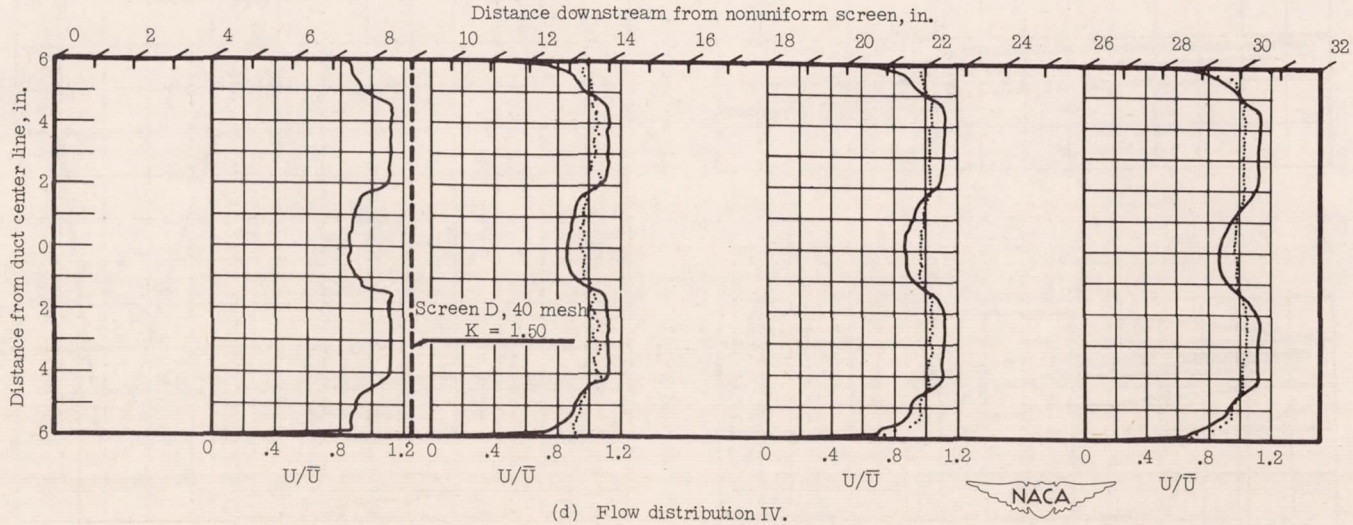

(d) Flow distribution IV.

Figure 14.- Concluded.

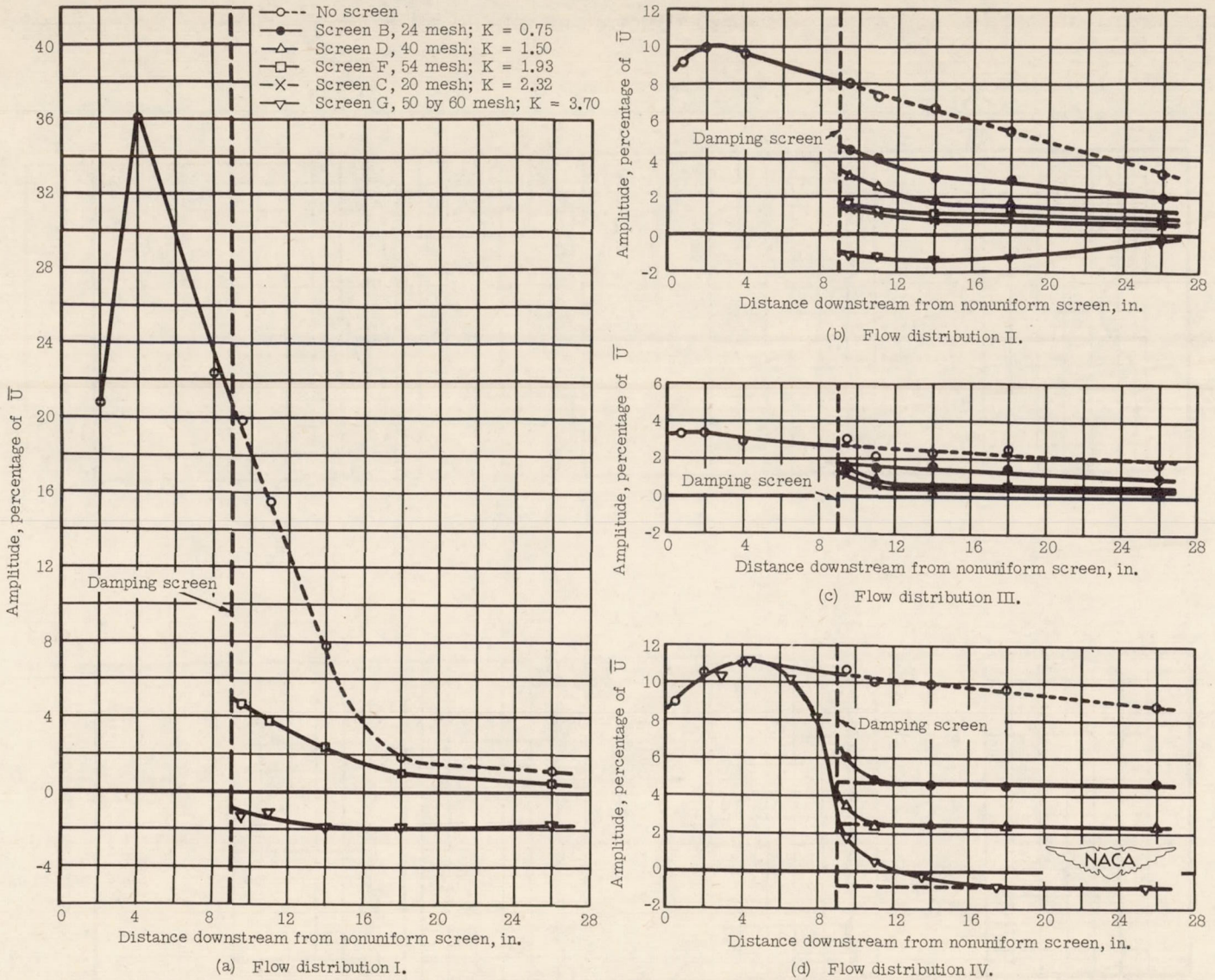

Figure 15.- Amplitude of spatial variations in speed as a function of distance along duct center line.

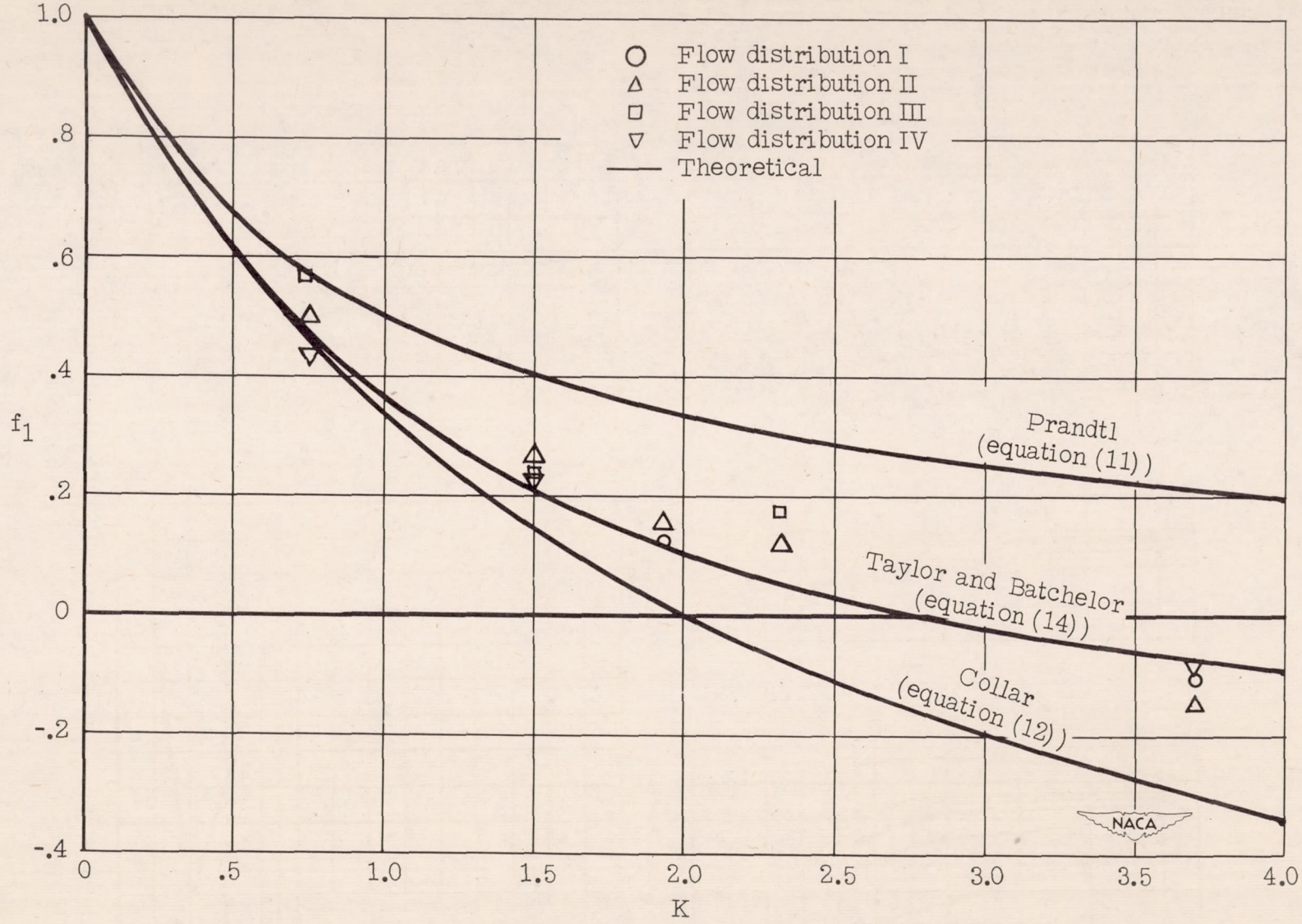

Figure 16.- Reduction factors for spatial variations in speed as a function of pressure-drop coefficient.